

# Thymopentapeptide Affects T-Cell Subsets by Modulating the Flora of the Skin Surface to Alleviate Psoriasis

Xin Liu<sup>1,\*</sup>, Ruofan Xi<sup>1,\*</sup>, Xinran Du<sup>1</sup>, Yi Wang<sup>1</sup>, Linyan Cheng<sup>1</sup>, Ge Yan<sup>1</sup>, Hanzhi Lu<sup>1</sup>, Te Liu<sup>2</sup>, Fulun Li<sup>1</sup>

<sup>1</sup>Department of Dermatology, Yueyang Hospital of Integrated Traditional Chinese and Western Medicine, Shanghai University of Traditional Chinese Medicine, Shanghai, People's Republic of China; <sup>2</sup>Shanghai Geriatric Institute of Chinese Medicine, Shanghai University of Traditional Chinese Medicine, Shanghai, People's Republic of China

\*These authors contributed equally to this work

Correspondence: Te Liu; Fulun Li, Email liute1979@shutcm.edu.cn; drlifulun@163.com

**Background:** Psoriasis is a common chronic inflammatory skin condition. The emergence of psoriasis has been linked to dysbiosis of the microbiota on the skin surface and an imbalance in the immunological microenvironment. In this study, we investigated the therapeutic impact of topical thymopentin (TP5) on imiquimod (IMQ)-induced psoriasis in mice, as well as the modulatory influence of TP5 on the skin immune milieu and the skin surface microbiota.

**Methods:** The IMQ-induced psoriasis-like lesion mouse model was used to identify the targets and molecular mechanisms of TP5. Immunofluorescence was employed to identify differences in T-cell subset expression before and after TP5 therapy. Changes in the expression of NF- $\kappa$ B signaling pathway components were assessed using Western blotting (WB). 16S rRNA sequencing and network pharmacology were used to detect changes in the skin flora before and after TP5 administration.

**Results:** In vivo, TP5 reduced IMQ-induced back inflammation in mice. H&E staining revealed decreased epidermal thickness and inflammatory cell infiltration with TP5. Masson staining revealed decreased epidermal and dermal collagen infiltration after TP5 administration. Immunohistochemistry showed that TP5 treatment dramatically reduced IL-17 expression. Results of the immunoinfiltration analyses showed psoriatic lesions with more T-cell subsets. According to the immunofluorescence results, TP5 dramatically declined the proportions of CD4<sup>+</sup>, Th17, ROR<sup>+</sup>, and CD8<sup>+</sup> T cells. WB revealed that TP5 reduced NF- $\kappa$ B pathway expression in skin tissues from IMQ-induced psoriasis model mice. 16S rRNA sequencing revealed a significant increase in *Burkholderia* and *Pseudomonadaceae\_Pseudomonas* and a significant decrease in *Staphylococcaceae\_Staphylococcus*, *Aquabacterium*, *Herbaspirillum*, and *Balneimonas*. *Firmicutes* dominated the skin microbial diversity after TP5 treatment, while *Bacteroidetes*, *Verrucomicrobia*, *TM7*, *Proteobacteria*, *Actinobacteria*, *Acidobacteria*, *Gemmatimonadetes*, and other species dominated in the IMQ group.

**Conclusion:** TP5 may treat psoriasis by modulating the epidermal flora, reducing NF- $\kappa$ B pathway expression, and influencing T-cell subsets.

**Keywords:** psoriasis, thymopentin, 16S rRNA sequencing, T-cell subsets

## Introduction

Psoriasis is a common chronic inflammatory skin disease that seriously affects the physical health, mental health, and quality of life of patients and is a key issue that urgently needs to be addressed in clinical practice.<sup>1</sup> Psoriasis commonly occurs on the extensor surfaces of the limbs, scalp, and back and is characterized by red plaques covered with multiple layers of silvery-white scales. Psoriatic skin lesions can be clinically classified into four types: plaque psoriasis, pustular psoriasis, psoriatic arthritis, and erythrodermic psoriasis.<sup>2</sup>

The IL-23/Th17 immune axis is the main immunological pathway involved in the pathogenesis of psoriasis.<sup>3,4</sup> When IL-23 secreted by dendritic cells binds to its receptor, it can induce the proliferation and activation of Th17 cells and promote their maintenance.<sup>5</sup> Activated Th17 cells produce a range of cytokines, including IL-17A/F, IL-22, IL-26, IFN- $\gamma$ , and granulocyte-macrophage-stimulating factor (GM-CSF), among others.<sup>6</sup> These cytokines recruit neutrophils and other immune cells and drive the inflammatory response, with IL-17 being the most critical mediator of this process.<sup>7-9</sup> IL-17 levels can be increased by various types of cells, including Th17 cells,  $\gamma\delta^+$  T cells, CD8<sup>+</sup> T cells, and CD4<sup>+</sup> T cells.<sup>10-12</sup> As the number and fraction of IL-17-secreting cells increase, the level of circulating IL-17 and IL-17 levels in peripheral tissue rise synchronously. This increase in systemic IL-17 causes local and systemic inflammation. Peripheral IL-17 activates NF- $\kappa$ B signaling pathways in keratinocytes, leading to the release of proinflammatory cytokines. This step is crucial to the inflammatory response in psoriasis.<sup>13,14</sup> For the treatment of psoriasis, commonly used drugs include immunosuppressants,<sup>15</sup> glucocorticoids,<sup>16</sup> vitamin D derivatives,<sup>17</sup> and retinoids.<sup>18</sup> However, the use of these medications can lead to dependence, and they are ineffective with prolonged use. Therefore, it is an urgent clinical problem to find an effective drug that could be used for a long period of time.

The composition of the skin microbiota is strongly linked to inflammatory skin diseases, and aberrant immune activation caused by the microbiota is involved in the pathogenesis of autoimmune disorders such as atopic dermatitis, psoriasis, and acne.<sup>19</sup> Some data reveal that psoriatic lesions have considerable microbiological diversity.<sup>20</sup> Compared to normal skin, the bacterial community in psoriatic epidermis has less stability and there are fewer immunomodulatory bacteria, such as *Staphylococcus epidermidis* and *Propionibacterium acnes*, which may increase the abundance of *Staphylococcus aureus* and worsen Th17 axis-related skin inflammation.<sup>4</sup> The level of *Cutibacterium*, *Burkholderia* spp. is decreased in psoriatic skin and that of *Corynebacterium kroppenstedtii*, *Corynebacterium simulans*, *Neisseria* spp., and *Finnegoldia* spp. is increased in psoriatic skin in comparison to healthy skin.<sup>21,22</sup> In pitying and chronic plaque psoriasis, *Thickettsia* is the most prevalent phylum, and *Streptococcus* is the most common genus.<sup>23</sup> These investigations revealed that skin flora dysregulation is directly linked to an imbalance in the immune milieu in psoriasis lesions, particularly activation of the Th17 axis, which promotes an increase in cytokines such as IL-17A, IL-17F, and IL22 to aggravate inflammation.

Thymopentin (TP5) has been demonstrated to have significant immunomodulatory effects. In thymic secretions, TP-5 is a component of thymopoietin II. Thymopoietin II is a single polypeptide that is extracted from thymic hormones that contain 49 amino acids; nevertheless, a peptide chain of five amino acids performs the same physiological function as thymopoietin II and is hence known as thymic pentapeptide.<sup>24</sup> TP5 has significant immunomodulatory and antimicrobial effects according to several studies. For example, TP5 increases resistance to infection in mice infected with multidrug-resistant *Mycobacterium tuberculosis*, reduces the bacterial load in the lungs and spleen, and improves immune functions.<sup>25</sup> TP5 also induces T-cell differentiation, promotes T-lymphocyte subpopulation development, maturation, and activation, and normalizes the CD4<sup>+</sup>/CD8<sup>+</sup> T-cell ratio.<sup>26</sup> TP5 was likewise found to have substantial LPS-neutralizing activity, as well as the ability to block LPS attachment and intracellular inflammatory responses.<sup>27</sup>

In this study, we found that topical administration of TP5 could treat model mice with IMQ-induced psoriasis by decreasing the expression of NF- $\kappa$ B signaling pathway components, altering the number and proportion of immune cells, and decreasing the expression of IL-17. This study provides some evidence for the clinical application of TP5 in the treatment of psoriasis. In addition, high-throughput 16S rRNA sequencing of the skin flora revealed that TP5 improved the composition of microorganisms on the skin surface in a mouse model of psoriasis, which is beneficial and can prevent psoriasis recurrence.

## Materials and Methods

### Ethics Statements

All animal experiments were carried out strictly in accordance with the Guidelines for Ethical Review of Laboratory Animal Welfare of the General Administration of Quality Supervision, Inspection and Quarantine of the People's Republic of China. The protocol was approved by the Institutional Animal Care and Use Committee (IACUC) of Yueyang Integrated Chinese and Western Medicine Hospital (assurance number YYLAC-2022-154-1). Mice were anesthetized via inhalation of isoflurane and euthanized humanely by cervical dislocation.

## Animal Experiments

Fifteen four- to six-week-old specific pathogen-free BALB/c male mice weighing 18–22 g were purchased from Shanghai Jihui Laboratory Animal Breeding Co. (Shanghai, China). The mice were housed at 24 °C and 40–60% humidity with a 12/12-h light/dark cycle. The mice were divided into three groups: the WT group, the IMQ modeling group and the TP5 treatment group. All mice were allowed free access to water and food. The psoriasis mouse model was established as previously described.<sup>28</sup> Mouse dorsal hair (3 cm × 3 cm) was shaved prior to the experiment, and all IMQ and TP5 treatments were applied to the shaved dorsal area of mice. After the application of a topical dose of 62.5 mg of commercially available IMQ daily for 7 days, psoriasis mouse modeling cream (Aldara, 3 M Pharmaceuticals) was continued to administer to induce psoriasis in the IMQ and TP5 groups. Following successful modeling, mice in the TP5 group were treated for three days with 0.08 mg/kg TP-5 (Hainan Zhonghe Pharmaceutical Co., Ltd., China) topically. On day 0–day 10, photographs of the mouse skin lesions were obtained. The skin lesions of mice were photographed, and the psoriasis area and severity index (PASI) were scored independently by two researchers before daily treatments. Skin samples (3 cm × 3 cm) were collected immediately after sacrificed.

## Hematoxylin–Eosin Staining and Masson’s Trichrome Staining

Tissue samples were fixed in 4% paraformaldehyde, dehydrated, and embedded in paraffin. Thin 4 μm-thick slices were then excised using a paraffin slicer and placed on a glass slide. Subsequently, the slices were dewaxed with xylene, followed by dehydration in an ethanol gradient. The slides were then stained with hematoxylin and Masson’s trichrome and incubated at 25 °C for 5 min, differentiated with 1% hydrochloric acid/ethanol for 30s, immersed in light ammonia water for 1 min to cause the nuclei to turn blue, and finally rinsed with distilled water for 5 min. Eosin was then added and the samples were incubated at 25 °C for 2 min, followed by rinsing with distilled water for 2 min. Next, ethanol gradient decolorization was performed, followed by xylene permeation for 2 min. Finally, slides were sealed with neutral gum for microscopy.

## Immunohistochemistry (IHC)

The expression of IL-17 was determined by IHC. Briefly, 4-μm-thick skin sections were baked (65 °C, 120 min). Then, the sections were dewaxed with xylene and gradient rehydrated with alcohol. After being washed (2 times for 5 min each) with PBS, the skin sections were placed in sodium citrate antigen retrieval solution. Antigen retrieval was achieved by boiling the solution for 20 min. Again, the sections were washed (3 times, 5 min each time) with PBS. The endogenous peroxidase blocking agent was added to the sections after cooling, and the sections were incubated at room temperature for 10 min. After being washed with PBS (3 times for 5 min each), the skin sections were covered with 5% BSA solution and incubated for 30 min at room temperature. The primary antibody was dissolved in a 5% BSA solution. Each section was covered with primary antibody solution (approximately 100 μL/section) and incubated overnight at 4 °C. The sections were brought back to room temperature and washed (3 times for 5 min each) with PBS. Then, the secondary antibody solution was added to the sections. After incubation for 90 min, the sections were washed (3 times for 2 min each) with PBS. DAB solution was added to the sections, which were then counterstained with hematoxylin. After being appropriately washed, the sections were rehydrated and mounted. Anti-IL-17 rabbit pAb (GB11110; Servicebio, Wuhan, China) was used.

## Immune Infiltration Analysis

Immune cell infiltration was determined by using the R CIBERSORT package, which is a deconvolution algorithm that can evaluate the proportion of 22 infiltrating lymphocyte subsets in a large number of tissue samples.<sup>29</sup> Correlation analysis between different immune cells and between immune cells and hub genes was performed using the R package Corrplot to calculate the proportion of each immune cell in psoriasis skin tissue and compare it to that in normal skin tissue (GSE13355).<sup>30</sup> By applying the single-sample gene set enrichment analysis (ssGSEA) method from the R package GSVA,<sup>31</sup> we calculated the degree of infiltration of 28 immune cell types based on gene expression levels in 28 published immune cell gene sets and analyzed the Spearman correlation of Gene-ssGSEA using the R package corrplot. Finally, differentially expressed genes were identified by the Xcell package.<sup>32</sup>

## Immunofluorescence Staining

Briefly, all fresh tissues were soaked at 25 °C and fixed in 4% paraformaldehyde (Sigma–Aldrich, St. Louis, MO, United States) for 30 min. Subsequently, the tissues were subjected to ethanol gradient dehydration, paraffin embedded, sliced (at a thickness of 6 μm), and dewaxed in xylene. Next, the tissues were sealed at 37 °C for 30 min with immunohistochemical blocking solution (Beyotime Biotechnology, Zhejiang, China). The blocking solution was discarded, and the sections were then washed three times with immunohistochemical cleaning solution (Beyotime Biotechnology) at 25 °C for 5 min. A primary antibody was subsequently added, and the samples were incubated at 37 °C for 45 min; the sections were again rinsed three times with the cleaning solution at 25 °C for 5 min. Next, a secondary antibody was added, and the samples were incubated at 37 °C for 45 min. Finally, after cleaning the sections three times with the cleaning solution at 25 °C for 5 min, immunofluorescence sealing solution (Sigma–Aldrich) was added. The following antibodies were used: anti-IL-17 rabbit pAb (GB11110; Servicebio, Wuhan, China); anti-CD4 rabbit pAb (GB11064; Servicebio, Wuhan, China); IFN-γ (D3H2) XP<sup>®</sup> rabbit mAb (#8455; Cell Signaling Technology, Shanghai, USA); anti-ROR gamma antibody (ab113434; Abcam, Cambridge, UK); TCR gamma/delta monoclonal antibody (eBioGL3 (GL-3, GL3)); and Biotin, eBioscience<sup>™</sup> (13–5711-81; Thermo Fisher Scientific, California, USA).

## Western Blotting

Briefly, protein samples from each group were separated by 12% denaturing SDS–PAGE, and proteins were then transferred to a PVDF membrane (Millipore, Billerica, MA, United States). After the membranes were sealed and washed, primary antibodies were added, and the membranes were incubated for 45 min at 37 °C. After the membranes were thoroughly washed, secondary antibodies were added, and the membranes were incubated for 45 min at 37 °C. The membranes were then washed four times with TBST at 25 °C for 14 min each. Finally, the protein bands were visualized with ECL<sup>®</sup> enhanced chemiluminescence reagents (ECL kit; Pierce Biotechnology, Waltham, MA, United States), and the band density was assessed by densitometry. The following antibodies were used: anti-IKK alpha rabbit pAb (GB11292; Servicebio, Wuhan, China), anti-IKK beta rabbit pAb (GB115540; Servicebio, Wuhan, China), anti-phospho-NF-κB p65 (S536) rabbit pAb (GB113882; Servicebio, Wuhan, China), and anti-beta-actin mouse mAb (GB12001; Servicebio, Wuhan, China).

## Skin Microbiota Analysis

As previously described, fresh skin samples were collected to analyze the skin microbiota.<sup>33,34</sup> Bacterial genomic DNA was extracted from frozen samples stored at –80 °C. The V3 and V4 regions of the 16S rRNA gene were amplified by PCR using specific primers (forward: 5'-ACTCCTACGGGAGGCAGCA3'; reverse: 5'-GGACTACHVGGGTWTCTAAT-3'). High-throughput pyrosequencing of PCR amplicons was performed on an Illumina sequencing platform at Biomarker Technologies (Beijing, China).<sup>34</sup> Raw paired-end reads from the original DNA fragments were merged using FLASH32 and assigned to each sample according to unique barcodes. UCLUST in QIIME (v1.8.0) was used based on 97% sequence similarity. The tags were clustered into operational taxonomic units (OTUs). The α-diversity index was evaluated using Mothur v1.30. The diversity index was compared among samples by standardizing the number of sequences in each sample. OTU rank curves, rarefaction curves, and Shannon curves were constructed, and Shannon, Chao, Simpson, and abundance-based coverage estimator indices were calculated. For β-diversity analysis, heatmaps of RDA-identified key OTUs were generated and principal coordinate analysis, nonmetric multidimensional scaling, and the unweighted pair group method with arithmetic means were performed using QIIME v1.8.0. The linear discriminant analysis (LDA)-effect size method was used for quantitative analysis of biomarkers. The LDA-effect size method (LDA score >2.0), nonparametric factorial Kruskal–Wallis sum-rank test, and unpaired Wilcoxon rank-sum test were applied to identify taxa with significantly different abundances.

## Statistical Analysis

Statistical analyses were performed using GraphPad Prism software (version 8; GraphPad Software Inc., San Diego, CA), and statistical significance was defined as  $P < 0.05$ . At least five sets of repeated experiments were performed, and *n* values indicate the number of animals analyzed in each group. Comparisons between two groups were made using one-way ANOVA.

## Results

### Thymopentin Treatment Improves the Condition of IMQ-Induced Psoriasis-Like Skin Lesions

The effect of TP5 on skin inflammation in mice was assessed using the dorsal skin condition of IMQ model mice and TP5-treated mice. Compared to those in the IMQ model group, mice in the TP5 group had significantly decreased dorsal skin inflammation, erythema, size, and thickness, as well as cumulative PASI scores (Figure 1). The major pathological sign of psoriasis is epidermal thickness. H&E staining of mouse skin slices was used to measure keratinocyte proliferation, dyskeratosis, and epidermis thickness. The TP5 group had considerably fewer basal cell layer keratinocytes and a thinner epidermis than did the IMQ group (Figure 2A). The TP5-treated group had much less collagen infiltration in the epidermis and dermis than the IMQ group, as measured by Masson staining (Figure 2B). IL-17 is a key inflammatory component in psoriasis lesions; however, compared with IMQ treatment, TP5 treatment dramatically reduced epidermal IL-17 infiltration (Figure 2C). The differences in all three staining indicators were significant (Figure 2D–).

### Thymopentin Reduces IL-17 Release from Immune Cells in Mice with IMQ-Induced Psoriatic Inflammation

We used differential gene immunoinfiltration analysis of the GSE13355 dataset to identify TP5 target cells. Immunoinfiltration revealed a substantial correlation between psoriasis and T-cell subset activation (Figure 3A). Cibersort analysis revealed a significant increase in activated memory CD4 T cells and follicular helper T-cell populations in the psoriasis group. Conversely, there was a significant decrease in the number of naive CD4<sup>+</sup> T cells, resting memory CD4<sup>+</sup> T cells, and regulatory T cells in the psoriasis group (Figure 3B). SsgSEA revealed a noteworthy increase in T follicular helper cells, type 1 T helper cells, type 17 helper cells, and type 2 T helper cells within the skin lesions of psoriasis patients (Figure 3C). The X cell analysis results indicated a significant increase in the immune microenvironment score within the skin lesions of psoriasis patients (Figure 3D). Then, whether TP5 improves T cell subset activation regulates the immune milieu in psoriasis skin lesions in mice. Immunofluorescence revealed that the activation of IL-17<sup>+</sup>/ROR $\gamma$ <sup>+</sup> T cells, IL-17<sup>+</sup>/ $\gamma$  $\delta$ <sup>+</sup> T cells, IL-17<sup>+</sup>/IFN $\gamma$ <sup>+</sup> cells and CD4<sup>+</sup>/IFN $\gamma$ <sup>+</sup> cells was significantly lower in the TP5 group than in the IMQ group (Figure 4A–E). Furthermore, Western blotting revealed that the relative expression levels of critical proteins in the NF- $\kappa$ B signaling pathway, namely, p-p65, IKK- $\alpha$ , and IKK- $\beta$ , were considerably lower in the TP5 group than in the IMQ group (Figure 4F and G). These findings demonstrate that TP5 can regulate the release of IL-17 from inflammatory cells, such as ROR<sup>+</sup>  $\gamma$ T cells,  $\gamma$  $\delta$ T<sup>+</sup> cells, Th17 cells, and CD4<sup>+</sup> T cells, by inhibiting the NF- $\kappa$ B signaling pathway.

### Thymopentin Significantly Modulated Skin Microecology in an IMQ-Induced Psoriasis Mouse Model

Skin tissues from the normal, IMQ-treated, and TP5-treated groups were collected to assess the composition of the skin microbiota and the distribution of specific flora by sequencing the bacterial 16S rRNA v3+v4 region. After splicing and filtering the double-ended reads, a total of 2,609,338 pairs of reads were obtained, and a total of 2,405,197 clean tags were generated, with each sample generating at least 61,004 clean tags and an average of 100,216 clean tags (Supplementary Table 1). Using QIIME2 (2019.4) and Vsearch (v2.13.4\_linux\_x86\_64), the tags were grouped into OTUs based on 97% sequence similarity. The number of ASVS/OTUs in the IMQ group was significantly different from that in the TP5 group (Figure 5A). The WT group had 3770 unique OTUs, the IMQ group had 887 unique OTUs, and the TP5 group had 836 unique OTUs, with 22 OTUs overlapping (Figure 5B). By comparing the representative sequences of OTUs with the microbial reference database, each OTU can be classified according to species. Simultaneously, the community composition of each sample was estimated. QIIME software was used to generate species abundance tables at multiple taxonomic levels (Kingdom, Phylum, Class, Order, Family, Genus, and Species). R language tools were used to map the sample community structure at several taxonomic levels. Phylum-level analysis revealed that the abundance of Firmicutes microorganisms significantly increased in the skin of mice in the TP5 group compared with those in the IMQ group, while the abundances of Actinobacteria, Bacteroidetes, Acidobacteria, Chloroflexi, Gemmatimonadetes, Planctomycetes, Cyanobacteria, and TM7 microorganisms decreased (Figure 5C). Genus-level analysis

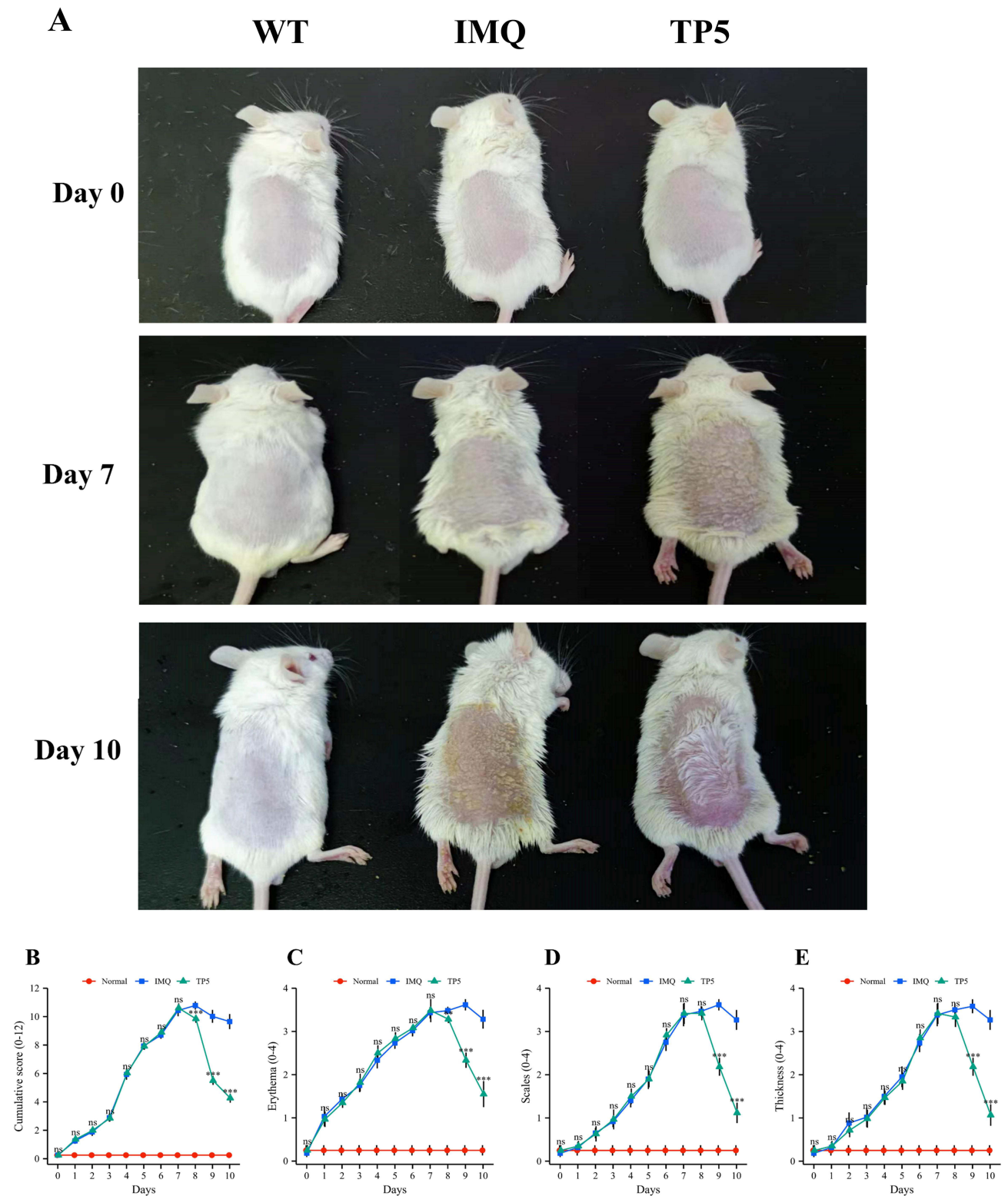


**Figure 1** TP5 ameliorates the psoriasis-like skin inflammation phenotype in IMQ-induced mice. **(A)** Phenotypic expression of genes in the dorsal skin of mice. Mice were divided into three groups, and each mouse was photographed before IMQ treatment and after TP5 treatment. **(B–E)** Line graphs showing cumulative PASI scores, skin erythema, desquamation and changes in skin thickness in mice. Each parameter was scored daily. The scores are expressed as the mean ± standard deviation. *ns*  $\geq 0.05$ , *\*\*\**  $P < 0.001$ , TP5 group vs IMQ group.

**Abbreviations:** IMQ, imiquimod; PASI, Psoriasis Area and Severity Index; TP5, thymopentin.

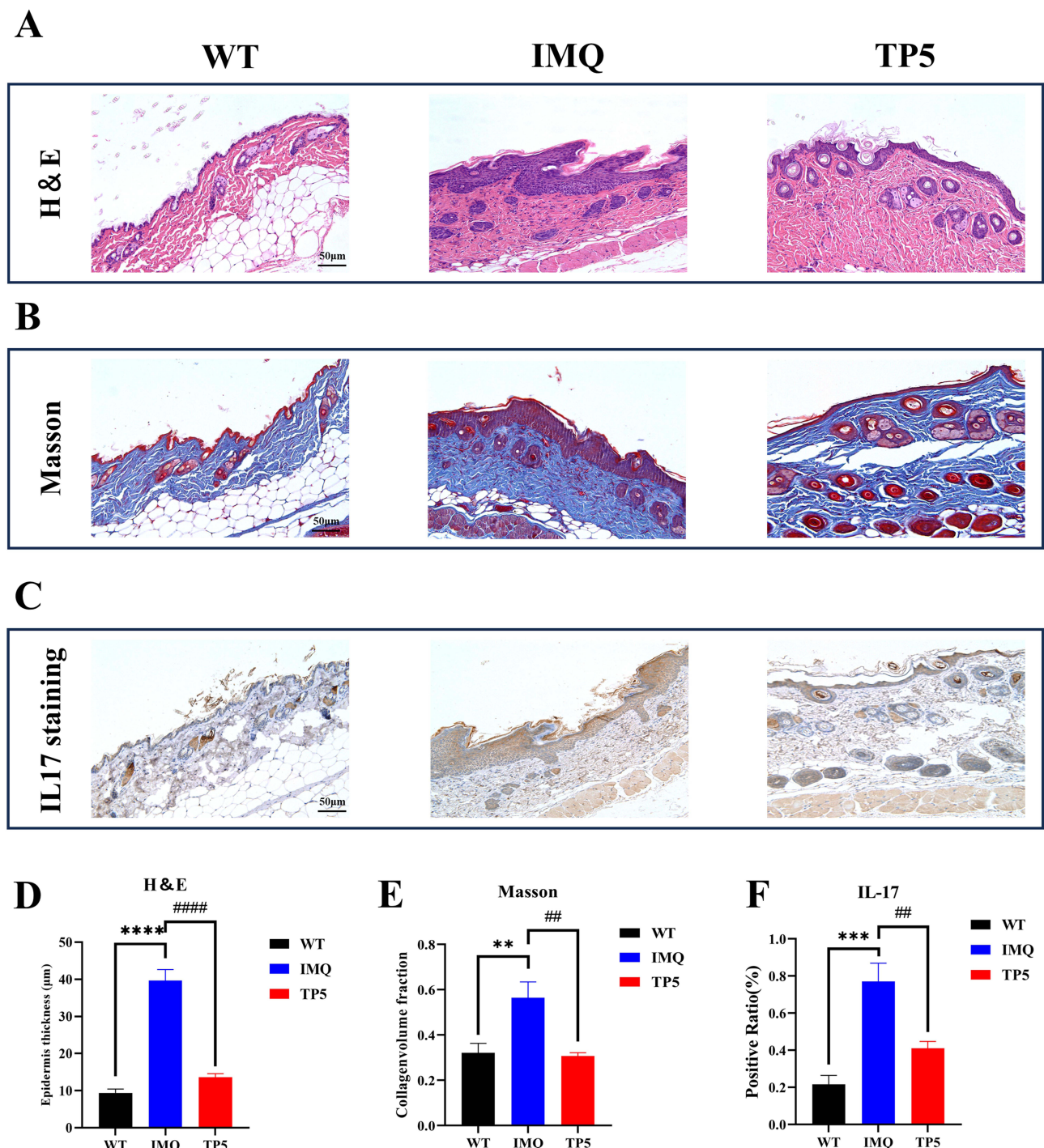


**Figure 2** TP5 alleviated the pathological features of psoriatic skin and reduced collagen infiltration and IL17 expression in the epidermis of psoriatic mice. **(A)** Representative images of H&E staining (scale bar = 50 µm). **(B)** Masson staining (scale bar = 50 µm). **(C)** IL-17 immunohistochemical staining (scale bar = 50 µm) of skin sections from mice in the WT, IMQ, and TP5 groups. **(D–F)** Statistical plots of epidermal layer thickness, the proportion of skin collagen, and the proportion of IL-17-positive skin sections from mice in the WT group, IMQ group, and TP5 group, as determined by H&E, Masson, and IHC staining. The scores are expressed as the mean ± standard deviation. \*\* $p < 0.01$ , \*\*\* $p < 0.001$ , \*\*\*\* $p < 0.0001$ , ## $p < 0.01$ , #### $p < 0.0001$ ; TP5 group vs IMQ group.

**Abbreviations:** IMQ, imiquimod; TP5, thymopentin.

revealed that *Burkholderia*, *Pseudomonadaceae\_Pseudomonas*, and *Planococcaceae\_Staphylococcus* microorganisms were significantly increased in the skin of mice in the TP5 group compared with those in the IMQ group, while the abundances of *Staphylococcaceae\_Staphylococcus*, *Aquabacterium*, *Herbaspirillum*, and *Balneimonas* were significantly decreased (Figure 5D). Species-level analysis revealed that *Burkholderia gladioli*, *Staphylococcus saprophyticus*, and *Faecalibacterium*

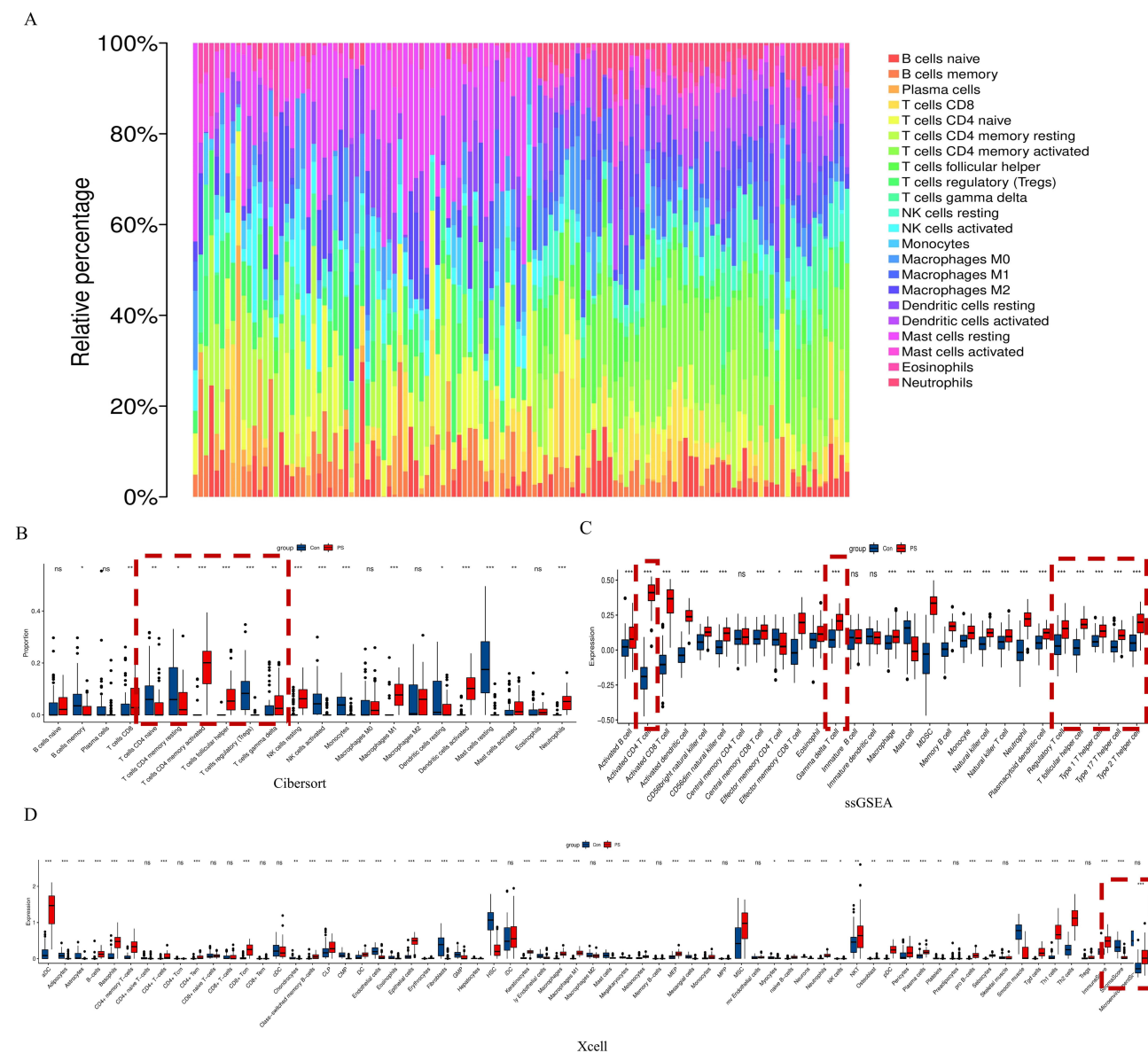


**Figure 3** GSE13355 transcriptome data mining predicted that TP5 altered the psoriasis immune microenvironment. **(A)** Immune infiltration analysis of DEGs between the normal group and the psoriasis group in the GSE13355 dataset. **(B)** CIBERSORT analysis of differentially expressed genes. **(C)** ssGSEA of differentially expressed genes. **(D)** X-cell analysis of differentially expressed genes.

*prausnitzii* were significantly more abundant in the skin of mice in the TP5 group than in that of mice in the IMQ group, while *Staphylococcus sciuri*, *Jeotgalicoccus psychrophilus*, and *Lactobacillus vaginalis* were significantly less abundant (Figure 5E). Cluster analysis revealed that most of the microbial diversity in the skin of mice in the TP5 group was attributable to Firmicutes (increased in number), Bacteroidetes, Verrucomicrobia, TM7, Proteobacteria, Actinobacteria, Acidobacteria, Gemmatimonadetes, etc. (Figure 5F and G).

The abundance rank curves from the alpha diversity study showed that the TP5 and IMQ groups had similar species abundances, while the WT group contained a more complex microbial community (Figure 6A). Species accumulation curves show that as the sample size increased, the curves changed from a sharp upward trend to a flat trend. This result indicates that the sample size of the sequencing data is large enough to reflect the species composition of the community (Figure 6B). The alpha diversity index analysis showed that there were no differences in the Chao 1, Faith<sub>pd</sub>, or Observed<sub>species</sub> indices between the skin microbes from mice in the TP5 and IMQ groups (Figure 6C), whereas there were significant differences in the Goods<sub>coverage</sub>, Shannon, Pieou<sub>e</sub>, and SimpsonS<sub>TPs</sub> indices (Figure 6D). Beta



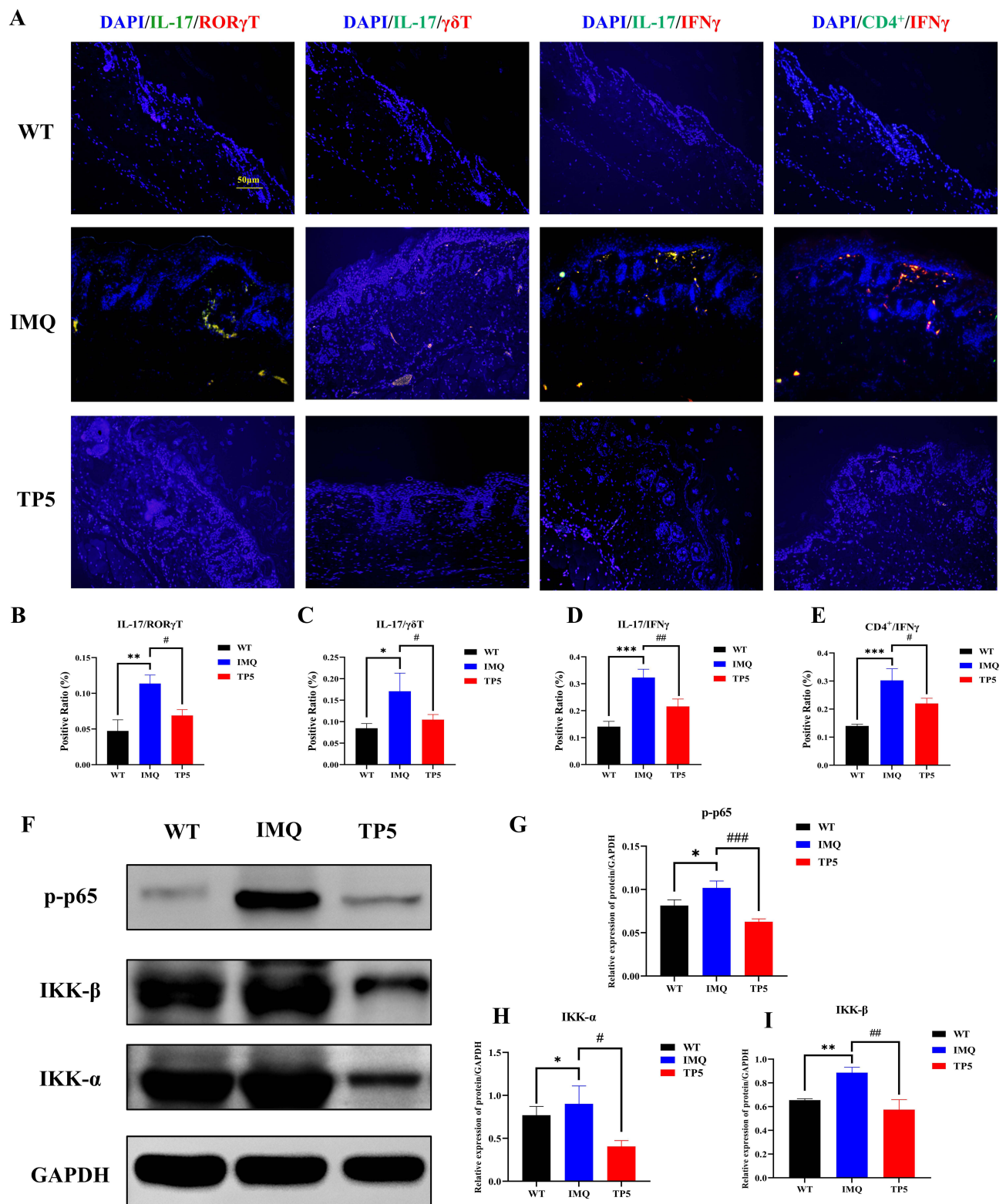


**Figure 4** Immunofluorescence staining showed that TP5 regulated the expression of T-cell subsets, and Western blotting results showed that TP5 decreased the expression of components of the NF- $\kappa$ B signaling pathway in skin tissues. (**A–E**) The proportions of IL-17<sup>+</sup>/ROR $\gamma$ T<sup>+</sup> T cells, IL-17<sup>+</sup>/ $\gamma$  $\delta$ T<sup>+</sup> T cells, IL-17<sup>+</sup>/IFN $\gamma$ <sup>+</sup> cells and CD4<sup>+</sup>/IFN $\gamma$ <sup>+</sup> cells were significantly lower in the skin sections of mice in the TP5 group than in those in the IMQ group, and the data are expressed as the mean  $\pm$  standard deviation. (**F–I**) The NF- $\kappa$ B signaling pathway-related proteins p-p65 and the relative protein expression levels of IKK- $\alpha$  and IKK- $\beta$  were determined by Western blotting. The data are expressed as the mean  $\pm$  standard deviation. \* $P$  < 0.05, \*\* $P$  < 0.01, \*\*\* $P$  < 0.001; # $P$  < 0.05, ## $P$  < 0.01, ### $P$  < 0.001.

**Abbreviations:** IMQ, imiquimod; TP5, thymopentin.

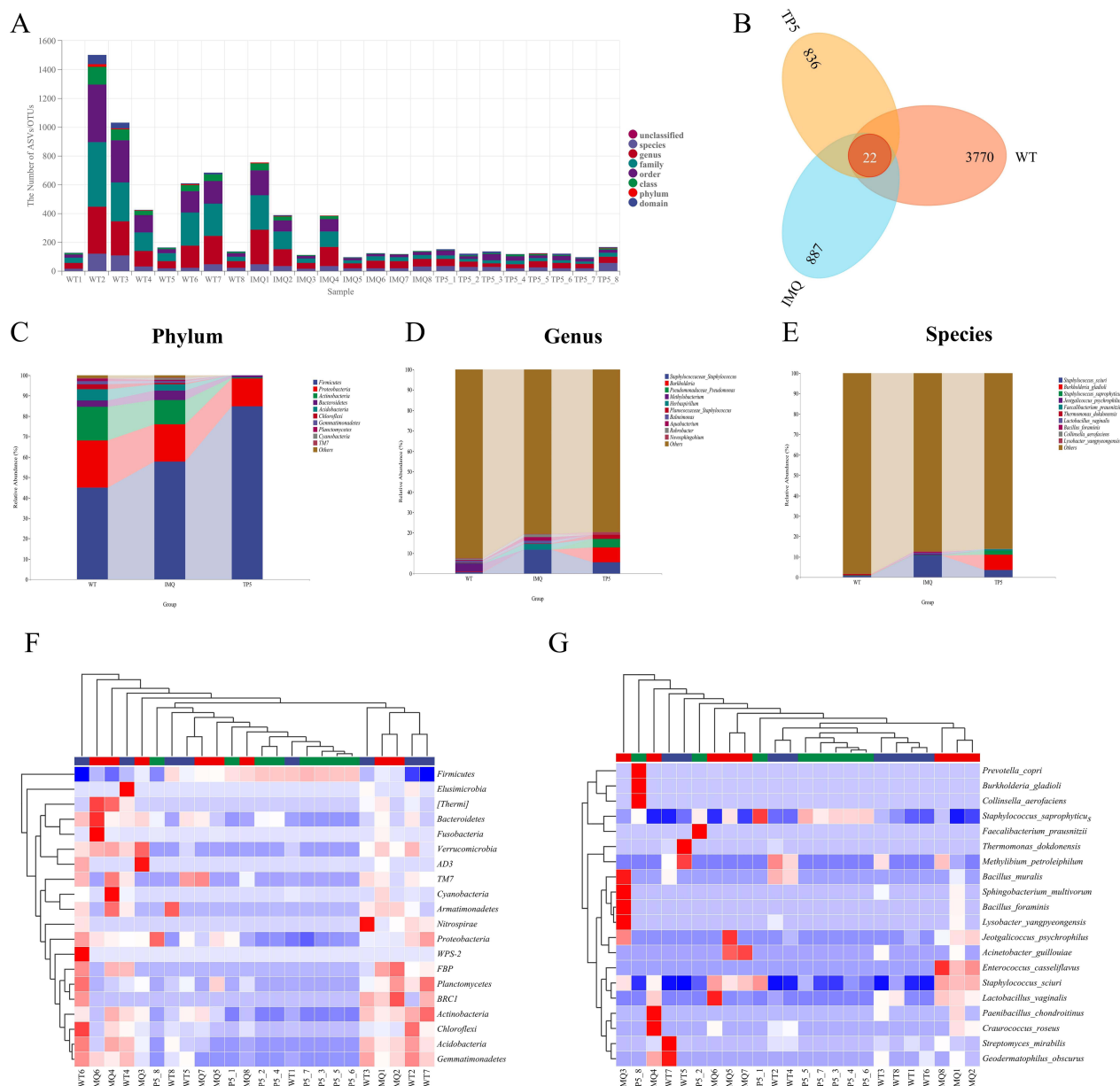


**Figure 5** Analysis of operational taxonomic units (OTUs) and a heatmap of species-richness clustering. **(A)** Number of OTUs. **(B)** Venn diagram of OTUs. **(C–E)** Skin microbiota clustering and species distribution at the phylum, genus and species levels. **(F)** Microbial diversity clustering in the phylum-level analysis. **(G)** Microbial diversity clustering in the species-level analysis.

diversity analysis was downscaled from multidimensional microbial data by unconstrained sorting methods such as principal coordinate analysis (PCoA) and nonmetric multidimensional scaling (NMDS), and by distributing the samples on successive sorting axes; in this manner, the main trends in data changes between the IMQ group and the TP5 group were demonstrated. The distance matrix and principal coordinates analysis were analyzed using the Jaccard algorithm, where the ellipse confidence level was set to 0.95, and the results revealed significant differences in microbial communities between the IMQ and TP5 groups (Figure 6E). Similarly, both OPLS-DA and PCA revealed differences in microorganisms at the species level in the IMQ and TP5 groups (Figure 6F and G). According to the results of the unweighted pair-group method with arithmetic mean (UPGMA) sample hierarchical clustering analysis, the skin microbiota of the IMQ group and the TP5 group were less homogeneous and did not share a similar genetic heritage (Figure 6H).

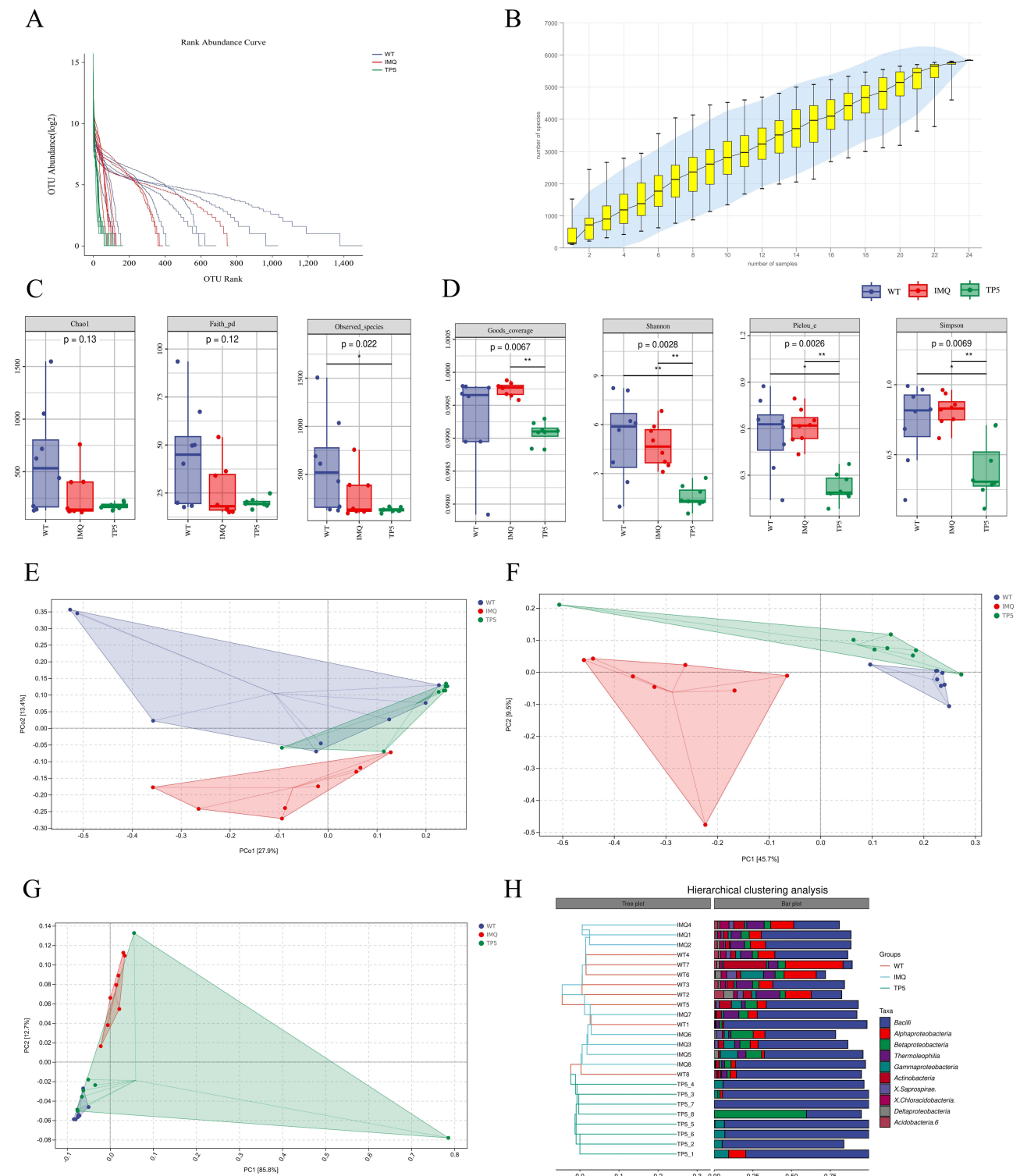


**Figure 6** Analysis of  $\alpha$  and  $\beta$  diversity. **(A)** Rank abundance curve. **(B)** Species accumulation curves. **(C)** Chao I, Faith's PD and observed species of alpha diversity analysis. **(D)** Good's coverage, Shannon, Pielou's evenness and Simpson indices were determined for alpha diversity analysis. **(E)** Results of the distance matrix and PCoA. **(F)** Results of orthogonal partial least squares discriminant analysis. **(G)** Results of principal coordinate analysis. **(H)** Unweighted-sample, pair-group method with arithmetic-mean clustering tree and combined illustration of the clustering tree and histogram.

Additionally, LDA effect size (LEfSe) was utilized to discover high-dimensional indicators in the skin microbiota of each group. The LDA score was 3.34, and species with LDA scores greater than 3.34 were deemed relevant biomarkers. According to the cladogram analysis and LDA score distribution, the IMQ group had a high number of p\_Bacteroidetes, c\_Rubrobacteria, c\_Bacteroidia and c\_Cytophagia microorganisms. In contrast, microorganisms such as p\_Firmicutes, c\_Bacilli, c\_Clostridia and c\_Betaproteobacteria were used as marker species in the TP5 group (Figure 7A). Microbial association networks were constructed to search for inherent patterns of co-occurrence or co-exclusion of specific microbial communities, driven by spatial and temporal variations and environmental processes (Figure 7B). Using Zi and Pi values, the nodes (ASVs/OTUs) in the network were divided into four parts, namely, peripherals, connectors, module hubs and network hubs, to identify hub or keystone species. According to the phylum classification, the bacterial community was dominated by Firmicutes, Proteobacteria, Actinobacteria, Bacteroidetes and Acidobacteria (Figure 7C).

## Thymopentin Dramatically Alters 16S Functional Gene Expression and Metabolic Signaling Pathways in the Skin of IMQ-Treated Mice

COG analysis was used to determine the distribution and abundance of homologous microbiota protein clusters (Supplementary Table 2). Overall, the microorganisms in each sample were mainly involved in amino acid biosynthesis (biosynthesis), nucleoside and nucleotide degradation (degradation/utilization/assimilation), antibiotic resistance (detoxification fermentation), metabolism (the Generation of Precursor Metabolites and Energy), fermentation (the generation of precursor metabolites and energy), glycan degradation (glycan pathways), nucleic acid processing (macromolecule modification) and pyrimidine deoxyribonucleotide phosphorylation (metabolic clusters) metabolic pathways (Figure 8A). KEGG metabolic pathway differential analysis allowed us to observe the differences and changes in functional gene metabolic pathways in microbial communities in samples from different subgroups, thereby allowing us to explore metabolic functional changes that occurred in different samples to adapt to environmental changes (Supplementary Table 3). The analysis revealed that the skin microbiota of the TP5 group exhibited an increase in proteins in the polymyxin resistance and nicotinate degradation I metabolism than did the skin microbiota of the IMQ group. However, the levels of proteins in the taurine breakdown pathway, the reductive TCA cycle II pathway, the ergothioneine biosynthesis I pathway (bacteria), and the UDP-N-acetylglucosamine-derived O-antigen building component biosynthesis metabolism pathway decreased (Figure 8B). After identifying metabolic pathways with differentially expressed proteins, we used R language tools to analyze the differences in

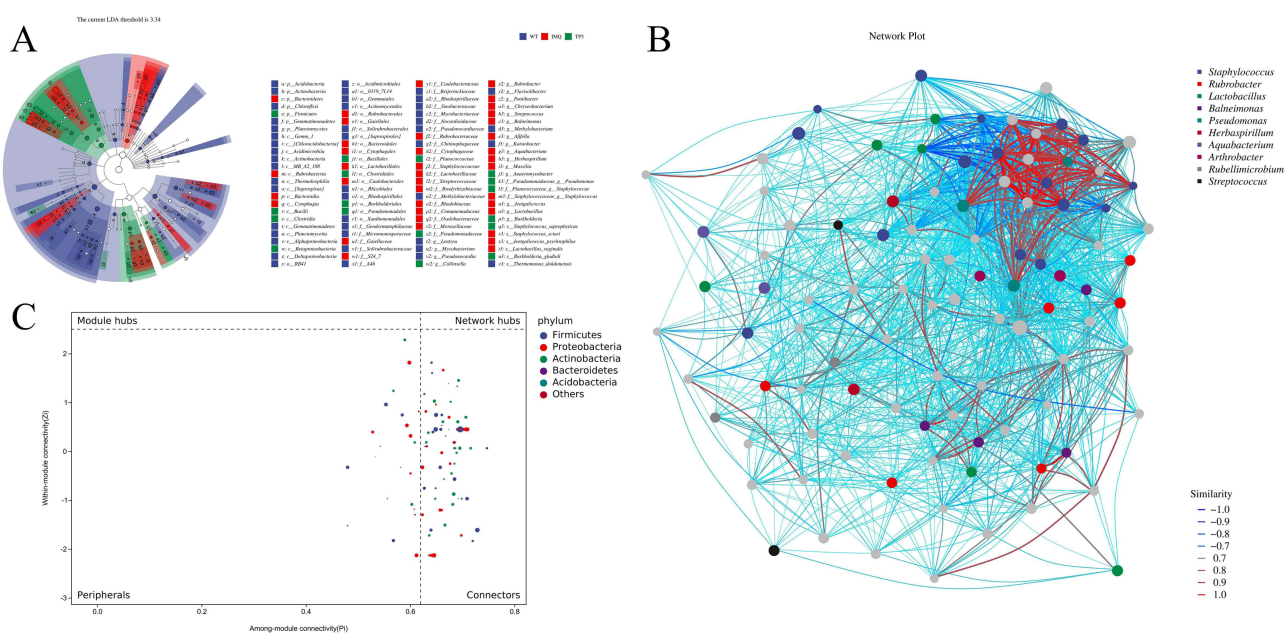


**Figure 7** Analysis of significant differences between groups. **(A)** Value-distribution histogram of the linear discriminant analysis effect size (LEfSe). **(B)** Species network at the ASV/OTU level. **(C)** ZIPI charts for ASVs/OTUs.

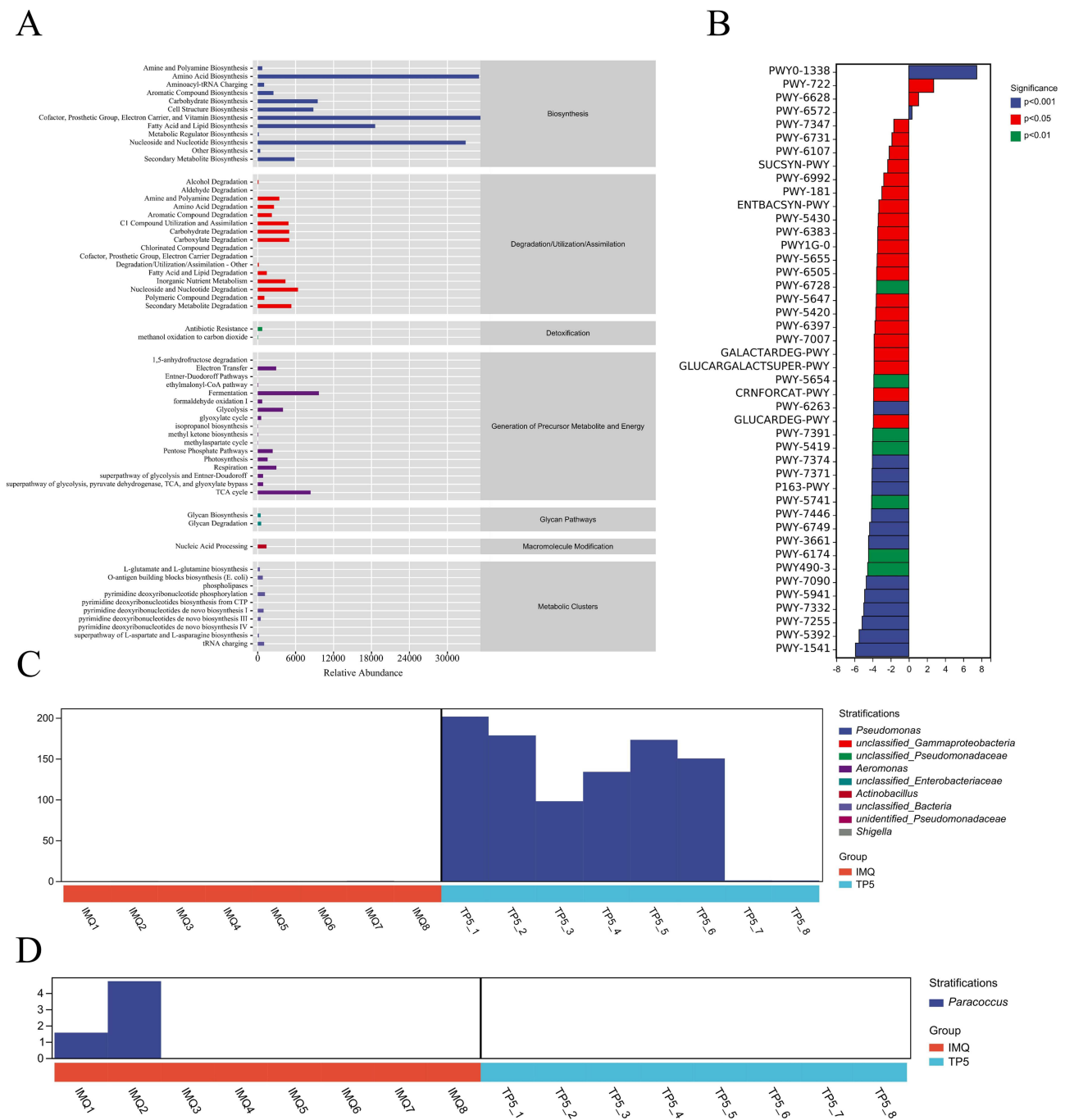


**Figure 8** Metabolic signaling pathways and protein differences in the skin microbiota. **(A)** Clusters of orthologous groups following analysis of the distributions and abundances of homologous protein clusters in pulmonary microbiota. **(B)** Results of Kyoto Encyclopedia of Genes and Genomes (KEGG) metabolic pathway analysis. **(C)** Differences in polymyxin resistance at the genus level. **(D)** Differences in the taurine degradation pathway at the genus level.

bacterial populations in terms of polymyxin resistance and the taurine degradation super pathway at the genus level (Figure 8C and D). According to these findings, TP5 reduced the abundance of bacteria such as *Pseudonocardia*, *Mycobacterium*, *Geodermatophilus*, and *Streptomyces* in the skin tissues of IMQ model animals.

## Discussion

In the treatment of psoriasis, the development of polyclonal antibodies has made it possible for the onset of moderate to severe psoriasis to disappear “overnight”. However, in clinical practice, the onset of psoriasis itself carries many

comorbidities. Therefore, the development of combination drugs will help to reduce multiple drug use and drug interactions, and improve patient's adherence to treatment, health and quality of life.<sup>35</sup> And the development of comprehensive drugs needs to be based on an in-depth understanding of disease pathogenesis. Currently, skin flora dysbiosis is considered to be an important causative factor in the development of psoriasis.<sup>36</sup>

According to previous research, the skin microbiota is critical for the development and modulation of immunological and inflammatory responses in psoriasis.<sup>37</sup> Skin microorganisms may interact with innate immune agents (eg, antimicrobial peptides and Toll-like receptors) to boost T-cell populations, resulting in an immunological cascade response and, eventually, psoriasis.<sup>38</sup> As a result, controlling the homeostasis of the skin flora aids in the treatment and recovery of psoriasis patients. Thymopentin, a 5-kDa (49-amino-acid) immunomodulatory protein derived from bovine thymus, can impact T-cell development and activity and has a good therapeutic effect when used in inflammatory illnesses.<sup>39</sup> For example, one researcher discovered that subcutaneous injections of thymopentin dramatically alleviated the clinical symptoms of atopic dermatitis.<sup>40–42</sup> In patients with active rheumatoid arthritis, slow intravenous infusion of thymopentin can provide significant relief.<sup>43</sup> However, thymopentin has not been investigated as a psoriasis treatment.

As a result, the purpose of this study was to confirm the efficacy of thymopentin in the treatment of psoriasis. We targeted the key immune cells that produce IL-17 because it is a prominent cytokine that is implicated in the pathogenesis of psoriasis. Animal experiments revealed that TP5 could improve the condition of skin lesions in the IMQ model mice, and H&E staining revealed that TP5 could reduce the thickness of the epidermis in the IMQ model mice. Masson staining revealed that TP5 could reduce collagen infiltration in the epidermis of the IMQ model mice and promote epidermal repair. Immunohistochemical staining revealed that IL-17 expression in the TP5 group was much lower than that in the IMQ group. To be more relevant to the Clinical setting, we analysed the differential genes in the GSE13355 dataset and performed immunoinfiltration analyses. The results of the analysis revealed that T-cell subsets were significantly elevated in skin lesion expression in patients with psoriasis. Since we did not conduct a clinical trial, we thus wanted to observe whether TP5 could reduce IMQ-induced high infiltration of T cells in the back of mice in a mouse model. We used immunofluorescence to assess the expression of immune cell surface markers, such as ROR $\gamma^+$  T cells,  $\gamma\delta^+$  T cells, Th17 cells, and CD4 $^+$  T cells, to determine whether TP5 reduced IL-17-associated inflammatory cell activation. According to the immunofluorescence data, the numbers of ROR $\gamma^+$  T cells,  $\gamma\delta^+$  T cells, Th17 cells, and CD4 $^+$  T cells and the levels of the immunomarkers IL-17/ROR $\gamma$ , IL-17/ $\gamma\delta$ , IL-17/IFN $\gamma$  and CD4/IFN $\gamma$  were considerably lower in the TP5 group than in the IMQ group. The relative expression level of p-p65 in the NF- $\kappa$ B signaling pathway was lower in the TP5 group than in the IMQ group, whereas the expression of the IKK- $\alpha$  protein was greater in the TP5 group than in the IMQ group, according to Western blotting data. We hypothesize that TP5 reduces epidermal immune cell infiltration by blocking the NF- $\kappa$ B signaling pathway. Thus, TP5 could have a possible molecular biological basis for the treatment of IMQ model mice and modulating IL-17-associated T-cell immunoreactivity.

After determining the phenotype, our next goal was to determine the molecular mechanism of TP5 therapy in IMQ model mice. TP5 was topically absorbed percutaneously for the treatment of psoriasis in this study. Given that the stability of the skin flora has a significant impact on the epidermis of psoriasis patients, we used high-throughput 16S rRNA sequencing to investigate whether there were any differences in flora colonization between WT mice, IMQ mice, and TP5 mice and what kind of differences were caused by these alterations. A varied and complex community of bacteria, fungi, viruses, archaea, and mites lives on healthy human skin, and the skin microbiota is composed mainly of *Malassezia*, *Keratobacterium*, *Aspergillus*, *Cryptococcus*, *Azospirillum*, and *Epicoccus*.<sup>44</sup> Changes in the number and composition of healthy skin microbiota cause an ecological imbalance in the skin, resulting in chronic inflammation and the generation of inflammatory factors that contribute to psoriasis. At the portal level, the relative abundance of *Bacteroides thickeniensis* increased in psoriatic skin, although the abundances of Actinobacteria and *Aspergillus* spp. differed.<sup>45</sup> At the genus level, streptococci and staphylococci were more abundant in lesional skin, with *Staphylococcus aureus* and *Streptococcus pyogenes* playing important roles in the pathogenesis of psoriasis.<sup>20</sup> The abundance of Staphylococcaceae\_Staphylococcus, Aquabacterium, Herbaspirillum, Balneimonas, and other psoriasis-promoting species decreased significantly in the TP5 treatment group, whereas that of Burkholderia Pseudomonadaceae\_Pseudomonas, Planococcaceae\_Staphylococcus, and other species that favour epidermal homeostasis increased significantly. Furthermore, cluster analysis revealed that in the TP5 group, genera such as Firmicutes, Bacteroidetes, Verrucomicrobia, TM7, Proteobacteria, Acidobacteria and Gemmatimonadetes were the species, with significantly higher abundance, and these species enhanced skin barrier function. The remaining microbiota

such as staphylococcus and Actinobacteria, which are damaging to the skin barrier, were reduced in abundance. Overall, our findings suggest that TP5 has pharmacological effects by regulating psoriasis-associated flora.

Finally, there has been no previous studies to investigated topical TP5 treatment for psoriasis, and we employed this treatment for the first time with some success in the IMQ mouse model; thus, these results provide some guidelines for topical TP5 treatment for psoriasis. However, our study has several limitations, including the following: we used glycerol to increase the adhesion of topical TP5 treatment, but its true absorption and utilization are unknown; we only used a single oral dose of TP5, and the difference in measured concentration has not been thoroughly studied.

However, in this work, we attempted to determine whether TP5 might regulate immunological imbalance and enhance the IMQ-induced inflammatory response by regulating changes in the skin flora. As a result, in the follow-up trial, we will experiment with different doses to determine the best topical dose of TP5. Furthermore, most investigations on TP5 as an immunomodulator have focused on its proinflammatory effects, with few studies investigating its impact on reducing inflammation and restoring immune system balance. We believe that TP5 is a promising medication that can be used to reduce chronic inflammation, and its regulatory mechanism should be investigated further.

## Conclusion

We suggest that TP5 achieves therapeutic effects in psoriasis by modulating the skin surface flora and influencing the NF- $\kappa$ B pathway to regulate the release of IL-17 from T-cell subsets.

## Data Sharing Statement

The datasets generated during and/or analyzed during the current study are available from the corresponding author on reasonable request.

## Acknowledgments

We acknowledge the support of Yueyang Hospital of Integrated Traditional Chinese and Western Medicine and Shanghai Geriatric Institute of Chinese Medicine. We are grateful to Wanjun Guo and Jianyong Zhu for their contribution to this article.

## Author Contributions

All authors contributed to data analysis, drafting or revising the article, have agreed on the journal to which the article will be submitted, gave final approval of the version to be published, and agree to be accountable for all aspects of the work.

## Funding

This research was funded by the Innovative Team Projects of Shanghai Municipal Commission of Health (2022CX011), Evidence-Based Capacity Building for TCM Specialty Therapies for Skin Diseases of National Administration of TCM, the Ministry of Education Chang Jiang Scholars Program, Young Qi-Huang Scholar of National Administration of Traditional Chinese Medicine, Youth Oriental Talent Program of Shanghai, High-level Chinese Medicine Key Discipline Construction Project (Integrative Chinese and Western Medicine Clinic) of National Administration of TCM (zyydxk-2023065), Shanghai Municipal Commission of Science and Technology 23Y31920300.

## Disclosure

The authors declare that the research was conducted in the absence of any commercial or financial relationships that could be construed as potential conflicts of interest.

## References

1. Lebwohl M. Advances in biologic therapy of psoriasis. *J Eur Acad Dermatol Venereol*. 2023;37(9):1689–1690. doi:10.1111/jdv.19287
2. Subedi S, Gong Y, Chen Y, et al. Infliximab and biosimilar infliximab in psoriasis: efficacy, loss of efficacy, and adverse events. *Drug Des Devel Ther*. 2019;13:2491–2502. doi:10.2147/DDDT.S200147
3. McDonald BD, Jabri B, Bendelac A. Diverse developmental pathways of intestinal intraepithelial lymphocytes. *Nat Rev Immunol*. 2018;18(8):514–525. doi:10.1038/s41577-018-0013-7

4. Chang HW, Yan D, Singh R, et al. Alteration of the cutaneous microbiome in psoriasis and potential role in Th17 polarization. *Microbiome*. 2018;6(1):154. doi:10.1186/s40168-018-0533-1
5. Navarro-Compan V. The paradigm of IL-23-independent production of IL-17F and IL-17A and their role in chronic inflammatory diseases. *Front Immunol*. 2023;14:1191782. doi:10.3389/fimmu.2023.1191782
6. Whitley SK, Li M, Kashem SW, et al. Local IL-23 is required for proliferation and retention of skin-resident memory TH17 cells. *Sci Immunol*. 2022;7(77):eabq3254. doi:10.1126/sciimmunol.abq3254
7. Sun R, Hedl M, Abraham C. IL23 induces IL23R recycling and amplifies innate receptor-induced signalling and cytokines in human macrophages, and the IBD-protective IL23R R381Q variant modulates these outcomes. *Gut*. 2020;69(2):264–273. doi:10.1136/gutjnl-2018-316830
8. Fu Y. Transcriptomic study on ovine immune responses to fasciola hepatica infection. *PLoS Negl Trop Dis*. 2016;10(9):e0005015. doi:10.1371/journal.pntd.0005015
9. Yang C. STAT4: an immunoregulator contributing to diverse human diseases. *Int J Biol Sci*. 2020;16(9):1575–1585.
10. Chen K, Eddens T, Trevejo-Nunez G, et al. IL-17 receptor signaling in the lung epithelium is required for mucosal chemokine gradients and pulmonary host defense against *K. pneumoniae*. *Cell Host Microbe*. 2016;20(5):596–605. doi:10.1016/j.chom.2016.10.003
11. Lang T, Lee JPW, Elgass K, et al. Macrophage migration inhibitory factor is required for NLRP3 inflammasome activation. *Nat Commun*. 2018;9(1):2223. doi:10.1038/s41467-018-04581-2
12. Dutzan N, Kajikawa T, Abusleme L, et al. A dysbiotic microbiome triggers TH17 cells to mediate oral mucosal immunopathology in mice and humans. *Sci Transl Med*. 2018;10(463). doi:10.1126/scitranslmed.aat0797
13. Kobayashi T, Naik S, Nagao K. Choreographing immunity in the skin epithelial barrier. *Immunity*. 2019;50(3):552–565. doi:10.1016/j.immuni.2019.02.023
14. Liu C, Liu H, Lu C, et al. Kaempferol attenuates imiquimod-induced psoriatic skin inflammation in a mouse model. *Clin Exp Immunol*. 2019;198(3):403–415. doi:10.1111/cei.13363
15. Zhang L, Guo L, Wang L, et al. The efficacy and safety of tofacitinib, peficitinib, solcitinib, baricitinib, abrocitinib and deucravacitinib in plaque psoriasis - A network meta-analysis. *J Eur Acad Dermatol Venereol*. 2022;36(11):1937–1946. doi:10.1111/jdv.18263
16. Muddasani S, Fleischer AB, Feldman SR. Treatment practices for psoriasis and how they are changing. *J Am Acad Dermatol*. 2021;84(2):579–581. doi:10.1016/j.jaad.2020.09.064
17. Hahn J, Cook NR, Alexander EK, et al. Vitamin D and marine omega 3 fatty acid supplementation and incident autoimmune disease: VITAL randomized controlled trial. *BMJ*. 2022;376:e066452. doi:10.1136/bmj-2021-066452
18. Lebowhl MG, Stein Gold L, Papp K, et al. Long-term safety and efficacy of a fixed-combination halobetasol propionate 0.01%/tazarotene 0.045% lotion in moderate-to-severe plaque psoriasis: Phase 3 open-label study. *J Eur Acad Dermatol Venereol*. 2021;35(5):1152–1160. doi:10.1111/jdv.17113
19. Rendon A, Schakel K. Psoriasis Pathogenesis and Treatment. *Int J Mol Sci*. 2019;20(6):1475. doi:10.3390/ijms20061475
20. Fahlen A, Engstrand L, Baker BS, et al. Comparison of bacterial microbiota in skin biopsies from normal and psoriatic skin. *Arch Dermatol Res*. 2012;304(1):15–22. doi:10.1007/s00403-011-1189-x
21. Olejniczak-Staruch I, Ciężńska M, Sobolewska-Sztychny D, et al. Alterations of the skin and gut microbiome in psoriasis and psoriatic arthritis. *Int J Mol Sci*. 2021;22(8):3998. doi:10.3390/ijms22083998
22. Alekseyenko AV, Perez-Perez GI, De Souza A, et al. Community differentiation of the cutaneous microbiota in psoriasis. *Microbiome*. 2013;1(1):31. doi:10.1186/2049-2618-1-31
23. Fry L, Baker BS, Powles AV, et al. Is chronic plaque psoriasis triggered by microbiota in the skin? *Br J Dermatol*. 2013;169(1):47–52. doi:10.1111/bjd.12322
24. Zhang L, Wei X, Zhang R, et al. Design and Development of a Novel Peptide for Treating Intestinal Inflammation. *Front Immunol*. 2019;10:1841. doi:10.3389/fimmu.2019.01841
25. Yuan XL, Wen Q, Ni M-D, et al. Immune formulation-assisted conventional therapy on anti-infective effectiveness of multidrug-resistant *Mycobacterium tuberculosis* infection mice. *Asian Pac J Trop Med*. 2016;9(3):293–297. doi:10.1016/j.apjtm.2016.01.031
26. Han YR, Wang T-H, Gong W-P, et al. Clinical efficacy of a combination of thymopentin and antituberculosis drugs in treating drug-resistant pulmonary tuberculosis: meta analysis. *Ther Clin Risk Manag*. 2022;18:287–298. doi:10.2147/TCRM.S351317
27. Zhang L, Wei X, Zhang R, et al. C-Terminal amination of a cationic anti-inflammatory peptide improves bioavailability and inhibitory activity against LPS-induced inflammation. *Front Immunol*. 2020;11:618312. doi:10.3389/fimmu.2020.618312
28. Guo W-J, Wang Y, Deng Y. Therapeutic effects of the extract of Sancao Formula, a Chinese herbal compound, on imiquimod-induced psoriasis via cysteine-rich protein 61. *J Integr Med*. 2022;20(4):376–384. doi:10.1016/j.joim.2022.04.004
29. Newman AM, Liu CL, Green MR, et al. Robust enumeration of cell subsets from tissue expression profiles. *Nat Methods*. 2015;12(5):453–457. doi:10.1038/nmeth.3337
30. Bindea G, Mlecnik B, Tosolini M, et al. Spatiotemporal dynamics of intratumoral immune cells reveal the immune landscape in human cancer. *Immunity*. 2013;39(4):782–795. doi:10.1016/j.immuni.2013.10.003
31. Hanzelmann S, Castelo R, Guinney J. GSVA: gene set variation analysis for microarray and RNA-seq data. *BMC Bioinf*. 2013;14(1):7. doi:10.1186/1471-2105-14-7
32. Aran D, Hu Z, Butte AJ. xCell: digitally portraying the tissue cellular heterogeneity landscape. *Genome Biol*. 2017;18(1):220. doi:10.1186/s13059-017-1349-1
33. Burns EM, Ahmed H, Isedeh PN, et al. Ultraviolet radiation, both UVA and UVB, influences the composition of the skin microbiome. *Exp Dermatol*. 2019;28(2):136–141. doi:10.1111/exd.13854
34. Shinno-Hashimoto H, Hashimoto Y, Wei Y, et al. Abnormal composition of microbiota in the gut and skin of imiquimod-treated mice. *Sci Rep*. 2021;11(1):11265. doi:10.1038/s41598-021-90480-4
35. Camela E, Potestio L, Fabbrocini G, et al. The holistic approach to psoriasis patients with comorbidities: the role of investigational drugs. *Expert Opin Investig Drugs*. 2023;32(6):537–552. doi:10.1080/13543784.2023.2219387
36. Langan EA, Griffiths CEM, Solbach W, et al. The role of the microbiome in psoriasis: moving from disease description to treatment selection? *Br J Dermatol*. 2018;178(5):1020–1027. doi:10.1111/bjd.16081



37. Rigon RB, de Freitas ACP, Bicas JL, et al. Skin microbiota as a therapeutic target for psoriasis treatment: trends and perspectives. *J Cosmet Dermatol.* 2021;20(4):1066–1072. doi:10.1111/jocd.13752
38. Liang X, Ou C, Zhuang J, et al. Interplay between skin microbiota dysbiosis and the host immune system in psoriasis: potential pathogenesis. *Front Immunol.* 2021;12:764384. doi:10.3389/fimmu.2021.764384
39. Singh VK, Biswas S, Mathur KB, et al. Thymopentin and splenopentin as immunomodulators. *Current Status Immunol Res.* 1998;17(3):345–368. doi:10.1007/BF02786456
40. Leung DY, Hirsch RL, Schneider L, et al. Thymopentin therapy reduces the clinical severity of atopic dermatitis. *J Allergy Clin Immunol.* 1990;85(5):927–933. doi:10.1016/0091-6749(90)90079-J
41. Hsieh KH, Shaio MF, Liao TN. Thymopentin treatment in severe atopic dermatitis—clinical and immunological evaluations. *Arch Dis Child.* 1992;67(9):1095–1102. doi:10.1136/adc.67.9.1095
42. Roekevisch E, Spuls PI, Kuester D, et al. Efficacy and safety of systemic treatments for moderate-to-severe atopic dermatitis: a systematic review. *J Allergy Clin Immunol.* 2014;133(2):429–438. doi:10.1016/j.jaci.2013.07.049
43. Malaise MG, Franchimont P, Bach-Andersen R, et al. Treatment of active rheumatoid arthritis with slow intravenous injections of thymopentin. A double-blind placebo-controlled randomised study. *Lancet.* 1985;1(8433):832–836. doi:10.1016/S0140-6736(85)92205-6
44. Lee HJ, Kim M. Skin barrier function and the microbiome. *Int J Mol Sci.* 2022;23:21.
45. Visser MJE, Kell DB, Pretorius E. Bacterial dysbiosis and translocation in psoriasis vulgaris. *Front Cell Infect Microbiol.* 2019;9:7. doi:10.3389/fcimb.2019.00007

## Drug Design, Development and Therapy

Dovepress

### Publish your work in this journal

Drug Design, Development and Therapy is an international, peer-reviewed open-access journal that spans the spectrum of drug design and development through to clinical applications. Clinical outcomes, patient safety, and programs for the development and effective, safe, and sustained use of medicines are a feature of the journal, which has also been accepted for indexing on PubMed Central. The manuscript management system is completely online and includes a very quick and fair peer-review system, which is all easy to use. Visit <http://www.dovepress.com/testimonials.php> to read real quotes from published authors.

Submit your manuscript here: <https://www.dovepress.com/drug-design-development-and-therapy-journal>